Elasticity Solution for Stresses in a Sandwich Beam with Functionally Graded Core

Satchi Venkataraman*
San Diego State University, San Diego, California 92182
and
Bhavani V. Sankar†
University of Florida, Gainesville, Florida 32611-6250

Introduction

WEIGHT savings offered by sandwich constructions for structures that require high bending stiffness are significant. However, sandwich constructions have not been fully exploited in structural applications due to damage tolerance concerns. The core–face-sheet delamination is a major concern in sandwich construction. The stiffness discontinuity at the face sheet and core interface results in a large increase in shear stresses. Although the core material itself may be able to withstand very high shear stresses, the bond (or adhesive layer) at the interface could be relatively weaker resulting in interfacial delamination. Results from this study indicate that the interfacial shear stresses can be reduced by varying (functionally grading) the core properties through the thickness.

This Note presents the displacement and stress fields in a functionally graded core for a one-dimensional sandwich plate and compares them to that in a uniform core. The objective is to demonstrate the significant reduction in shear stresses at the face-sheet–core interface in the sandwich panel achieved by functionally grading the core properties.

Elasticity Analysis

The sandwich analysis proposed here is based on the elasticity analysis developed for a continuous functionally graded material (FGM) beam by Sankar.[1] For the sandwich beam analysis, we subdivide the beam in the thickness direction into four elements or layers as shown in Fig. 1. The layers will be referred to as the top and bottom face sheets and top and bottom halves of the sandwich core. Euler–Bernoulli beam theory is used to model the face sheets and plane elasticity equations are used to analyze the core. In this Note, we will provide only the details necessary to reproduce the results presented later. Details of the elasticity equations used to derive the model are presented in Ref. 1.

The governing equations are formulated separately for each element, and compatibility of displacements and continuity of tractions are enforced at each interface (node) to obtain the global equations, which are solved to obtain the displacement and stress fields in the individual layers of the sandwich beam. This procedure is analogous to assembling element stiffness matrices to obtain a global stiffness matrix in finite element analysis.

The face sheets are assumed to be homogeneous and isotropic. The core is functionally graded but symmetric about the midplane given by $z = 0$. The elasticity coefficients c_{ij} of the top half of the core are assumed to vary according to

$$c_{ij} = c_{ij}^{0} e^{\lambda z} \tag{1}$$

In the following sections, we will derive the equations for each element. The tractions and displacements at the interface between each element are shown in Fig. 1. Each element has its own local coordinate system.

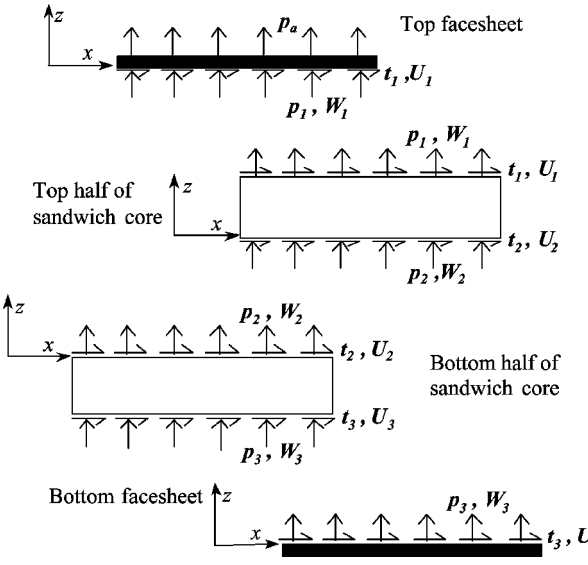

Fig. 1 Traction forces and displacements at the interfaces of each element in the FGM sandwich beam.

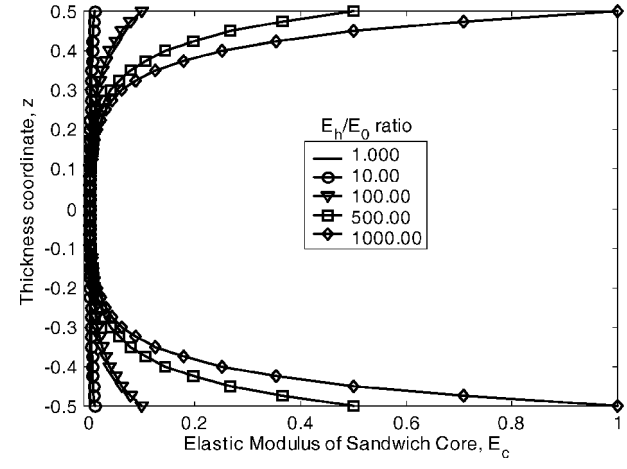

Fig. 2 Through-the-thickness variations of core modulus considered for the functionally graded sandwich beam (E_h, sandwich core modulus at the face-sheet interface; E_0, sandwich core modulus at center).

Top Face Sheet

The Euler–Bernoulli beam theory is used for the analysis of face sheets. This is admissible if the face sheet thickness is small (compared to beam length and core thickness) and, hence, the shear deformation can be neglected. The reference plane ($z = 0$) for the top face sheet is assumed to be along the face-sheet–core interface as shown in Fig. 2.

Let $t_1(x)$ and $p_1(x)$ be the shear and normal tractions that act at the bottom surface of the face sheet. The normal surface loads p_a acting on the top surface can be combined with the normal traction p_1. Our goal is to derive expressions for the displacements $u(x, 0)$ and $w(x)$ along the bottom surface of the beam in terms of t_1 and p_1.

The equilibrium equations for the beam are expressed as

$$\frac{dP}{dx} = -t_1(x) \tag{2}$$

Presented as Paper 2001-1281 at the 42nd Structures, Structural Dynamics, and Material Conference, Seattle, WA, 16–19 April 2001; received 5 September 2001; revision received 20 June 2003; accepted for publication 20 June 2003.

*Assistant Professor, Department of Aerospace Engineering and Engineering Mechanics. Member AIAA.
†Professor, Department of Mechanical and Aerospace Engineering. Associate Fellow AIAA.

$$\frac{\mathrm{d}^2M}{\mathrm{d}x^2} = \frac{\mathrm{d}V}{\mathrm{d}x} = -p_1 \tag{3}$$

where $P(x)$ is the axial force resultant, $V(x)$ is the shear force, and $M(x)$ is the bending moment along the length of the beam. Let the displacement field in the beam be of the form

$$u(x, z) = u_1(x) - z\frac{\mathrm{d}w_1}{\mathrm{d}x} \tag{4}$$

where $u_1(x)$ is the axial displacement of points on the bottom surface of the face sheet and $w_1(x)$ is the transverse deflection, which is independent of z. The constitutive relations of the laminate are of the form

$$\begin{Bmatrix} P \\ M \end{Bmatrix} = \begin{bmatrix} A & B \\ B & D \end{bmatrix} \begin{Bmatrix} \dfrac{\mathrm{d}u_1}{\mathrm{d}x} \\ \dfrac{-\mathrm{d}^2w_1}{\mathrm{d}x^2} \end{Bmatrix} \tag{5}$$

where the stiffness coefficients A, B, and D are defined as follows:

$$[A, B, D] = \int_0^{h_f} \bar{Q}_{11}(1, z, z^2)\,\mathrm{d}z \tag{6}$$

It should be noted that the limits of integration in Eq. (6) are 0 to h_f because we use the bottom surface of the face sheet as the reference surface. Substituting from Eq. (5) for P and M in the equilibrium equations (2) and (3), we obtain the governing differential equations for the top face sheet:

$$A\frac{\mathrm{d}^2u_1}{\mathrm{d}x^2} - B\frac{\mathrm{d}^3w_1}{\mathrm{d}x^3} = -t_1, \qquad B\frac{\mathrm{d}^3u_1}{\mathrm{d}x^3} - D\frac{\mathrm{d}^4w_1}{\mathrm{d}x^4} = -p_1 \tag{7}$$

We assume that the displacements and tractions are of the form

$$u_1(x) = U_1\cos(\xi x), \qquad w_1(x) = W_1\sin(\xi x)$$
$$t_1(x) = T_1\cos(\xi x), \qquad p_1(x) = P_1\sin(\xi x) \tag{8}$$

where U_1, W_1, T_1, and P_1 are constants to be determined.

The top face sheet is subjected to normal tractions such that

$$\sigma_{zz}(x) = P_{an}\sin(\xi x), \qquad \xi = n\pi/L, \qquad n = 1, 3, 5, \ldots \tag{9}$$

where P_{an} is a known constant. Since n is assumed odd-valued, the loading is symmetric about the center of the beam. The loading given by Eq. (9) is of practical significance because any arbitrary loading can be expressed as a Fourier series involving terms of the type $P_{an}\sin(\xi x)$.

$$\det\begin{bmatrix} \left(\dfrac{1-2\nu}{2}\right)\alpha^2 + \left(\dfrac{1-2\nu}{2}\right)\lambda\alpha - (1-\nu)\xi^2 & \dfrac{\xi\alpha}{2} + \left(\dfrac{1-2\nu}{2}\right)\lambda\xi \\ -\dfrac{\xi\alpha}{2} - \nu\lambda\xi & (1-\nu)\alpha^2 + (1-\nu)\lambda\alpha - \left(\dfrac{1-2\nu}{2}\right)\xi^2 \end{bmatrix} = 0 \tag{17}$$

Substituting from Eqs. (9) and (8) into Eq. (7) we obtain a relation between the interface displacements U_1, and W_1 and the tractions T_1 and P_1:

$$\left[K^{(1)}\right]\begin{Bmatrix} U_1 \\ W_1 \end{Bmatrix} = \begin{bmatrix} \xi^2A & -\xi^3B \\ -\xi^3B & \xi^4D \end{bmatrix}\begin{Bmatrix} U_1 \\ W_1 \end{Bmatrix} = \begin{Bmatrix} T_1 \\ P_1 + P_a \end{Bmatrix}^{(1)} \tag{10}$$

where $K^{(1)}$ can be considered the stiffness matrix of element 1, that is, the top face sheet. The superscripts on the right-hand side indicate that the tractions act on element 1.

Bottom Face Sheet

The equations of the bottom face sheet can be derived in a manner similar to that for the top face sheet. Following the procedures described in the preceding section, we obtain a relation for bottom face sheet as follows:

$$\left[K^{(4)}\right]\begin{Bmatrix} U_3 \\ W_3 \end{Bmatrix} = \begin{bmatrix} \xi^2A & -\xi^3B \\ -\xi^3B & \xi^4D \end{bmatrix}\begin{Bmatrix} U_3 \\ W_3 \end{Bmatrix} = \begin{Bmatrix} T_3 \\ P_3 \end{Bmatrix}^{(4)} \tag{11}$$

However, the definitions of A, B, and D are different from those used for the top face sheet because the reference surface for the bottom face sheet is at the top surface. The choice of reference surface results in the integration being performed from $-h_f$ to 0, thereby resulting in different values for the stiffness terms, which are given by

$$[A, B, D] = \int_{-h_f}^{0} \bar{Q}_{11}(1, z, z^2)\,\mathrm{d}z \tag{12}$$

Top Half of the Core

The functionally graded core is analyzed using the plane elasticity equations. The material is assumed to be pointwise isotropic but spatially varying. The exponential variation in the elastic coefficients in the z direction [Eq. (13)] are obtained by varying the elastic modulus and assuming a constant Poisson ratio:

$$[c(z)] = e^{\lambda z}\begin{bmatrix} c_{11}^0 & c_{13}^0 & 0 \\ c_{13}^0 & c_{33}^0 & 0 \\ 0 & 0 & c_{55}^0 \end{bmatrix} \tag{13}$$

where $c_{ij}^0 = c_{ij}(z = 0)$. The elasticity model developed earlier [Eqs. (1–16) from Ref. 1] is used to analyze the core. The elasticity model assumes a displacement field of the form

$$u(x, z) = U(z)\cos\xi x, \qquad w(x, z) = W(z)\sin(\xi x) \tag{14}$$

which satisfies simple support boundary conditions for the beam as follows:

$$w(0, z) = w(L, z) = 0, \qquad \sigma_{xx}(0, z) = \sigma_{xx}(L, z) = 0 \tag{15}$$

The displacement variations through the thickness $U(z)$ and $W(z)$ are of the form

$$U(z) = \sum_{i=1}^{4} a_i e^{\alpha_i Z}, \qquad W(z) = \sum_{i=1}^{4} b_i e^{\alpha_i Z} \tag{16}$$

where α_i are the roots of the following characteristic equation (obtained from the differential equations of equilibrium[1]):

Denote the x- and z-direction displacements at the top and bottom surfaces of element 2 by U_1, W_1, U_2, and W_2, respectively. Then the relation between these surface displacements and the constants $a_1, \ldots, a_4$ in solution (16) can be obtained as

$$\begin{Bmatrix} U_1 \\ W_1 \\ U_2 \\ W_2 \end{Bmatrix} = \begin{bmatrix} e^{\alpha_1 h/2} & e^{\alpha_2 h/2} & e^{\alpha_3 h/2} & e^{\alpha_4 h/2} \\ r_1 e^{\alpha_1 h/2} & r_2 e^{\alpha_2 h/2} & r_3 e^{\alpha_3 h/2} & r_4 e^{\alpha_4 h/2} \\ 1 & 1 & 1 & 1 \\ r_1 & r_2 & r_3 & r_4 \end{bmatrix}\begin{Bmatrix} a_1 \\ a_2 \\ a_3 \\ a_4 \end{Bmatrix}$$
$$= [M]\begin{Bmatrix} a_1 \\ a_2 \\ a_3 \\ a_4 \end{Bmatrix} \tag{18}$$

where r_i is the ratio of the arbitrary constants a_i and b_i in the displacement functions for $U(z)$ and $W(z)$:

$$r_i = \frac{b_i}{a_i} = -\frac{(1-2\nu)\alpha_i(\lambda+\alpha_i) - 2(1-\nu)\xi^2}{\xi\alpha + (1-2\nu)\lambda\xi} \tag{19}$$

The tractions t_1, p_1, t_2, and p_2 acting on the surface can be related to the stresses as follows:

$$\begin{Bmatrix} t_1 \\ p_1 \\ t_2 \\ p_2 \end{Bmatrix}^{(2)} = \begin{Bmatrix} \tau_{xz}(h/2) \\ \sigma_{zz}(h/2) \\ -\tau_{xz}(0) \\ -\sigma_{zz}(0) \end{Bmatrix} \tag{20}$$

Then using the stress–strain, strain-displacement, and constitutive relations we can express the surface tractions as a function of the unknown coefficients a_i:

$$\begin{Bmatrix} T_1 \\ P_1 \\ T_2 \\ P_2 \end{Bmatrix}^{(2)} = [S] \begin{Bmatrix} a_1 \\ a_2 \\ a_3 \\ a_4 \end{Bmatrix} \tag{21}$$

where

$$\begin{aligned} S_{1j} &= c_{55}^0 e^{\alpha_i h/2}\left(\alpha_j + \xi r_j\right) \\ S_{2j} &= e^{\alpha_i h/2}\left(-c_{11}^0\xi + c_{33}^0 r_j\alpha_j\right) \\ S_{3j} &= -c_{55}^0\left(\alpha_j + \xi r_j\right) \\ S_{4j} &= -\left(-c_{11}^0\xi + c_{33}^0 r_j\alpha_j\right), \qquad j = 1,4 \end{aligned} \tag{22}$$

The stiffness matrix of the top half of the FGM core $[K^{(2)}]$, which relates the surface tractions to the surface displacements, is obtained by combining Eqs. (21) and (18) and eliminating the coefficients a_i and is expressed as follows:

$$\left[K^{(2)}\right] \begin{Bmatrix} U_1 \\ W_1 \\ U_2 \\ W_2 \end{Bmatrix} = [S][M]^{-1} \begin{Bmatrix} U_1 \\ W_1 \\ U_2 \\ W_2 \end{Bmatrix} = \begin{Bmatrix} T_1 \\ P_1 \\ T_2 \\ P_2 \end{Bmatrix}^{(2)} \tag{23}$$

Bottom Half of the Core

The differential equilibrium and stress–strain relations are identical to those defined for the top half of the core. The reference surface for the z coordinate in the bottom half of the core is chosen at its top surface (midplane of the sandwich) and hence z values are negative. The similarities in geometry, loading, and the material property variations between the top and bottom half of the sandwich core permit us to obtain the stiffness matrix for the bottom half of the core by means of a simple geometric transformation given by

$$\left[K^{(3)}\right] = [T]^{-1}\left[K^{(2)}\right][T] \tag{24}$$

where the transformation matrix T is of the form

$$T = \begin{bmatrix} 0 & 0 & 1 & 0 \\ 0 & 0 & 0 & -1 \\ 1 & 0 & 0 & 0 \\ 0 & -1 & 0 & 0 \end{bmatrix} \tag{25}$$

Assembling the Elements

To satisfy equilibrium, the contributions of tractions from different elements at each interface should sum to zero. Enforcing the compatibility of displacements at the interfaces enables us to assemble the stiffness matrices of the four elements to obtain a global stiffness matrix K:

$$[K] \begin{Bmatrix} U_1 \\ W_1 \\ U_2 \\ W_2 \\ U_3 \\ W_3 \end{Bmatrix} = \begin{Bmatrix} 0 \\ P_{an} \\ 0 \\ 0 \\ 0 \\ 0 \end{Bmatrix} \tag{26}$$

The displacements U_i and W_i are obtained by solving Eq. (26). Then the complete displacement field in an element can be obtained using Eqs. (16–18) and the stresses from the corresponding constitutive relations.

Results and Discussion

The length of the beam is denoted by L, the core thickness by h, and the face-sheet thicknesses by h_f. Sandwich-beam results presented here correspond to a beam $L/h = 10$ and $h_f/h = 0.1$. The face-sheet elastic modulus is chosen at an arbitrary value of 1.0. We restrict our study to the case where the beam is loaded in the transverse direction by a sinusoidal load given by $p_a \sin(\pi x/L)$. The chosen load magnitude is $p_a/E_f = 10^{-2}$. The sandwich core modulus at the midplane is kept fixed at $E_f/1000$ while the core modulus at the face-sheet interface, E_h, is varied. The ratio of E_h/E_0 varies from 1 to 1000. When $E_h/E_0 = 1$, core properties are constant through the thickness and identical to a regular sandwich panel. The value of E_h is gradually increased until it reaches the value of the face sheet for $E_h/E_0 = 1000$. The different profiles of the elastic modulus variations in the sandwich core are shown in Fig. 2. The displacements through the thickness of the sandwich core are plotted in Figs. 3 and 4, respectively. The bending stresses, normal stress (core compression), and shear stress are plotted in Figs. 5, 6, and 7, respectively.

The in-plane displacement (Fig. 3) exhibits a nonlinear variation through the thickness of the core for the functionally graded core sandwich, significantly different from that observed in homogeneous sandwich cores. The elasticity solution also provides the compressions of the sandwich core in its thickness direction, which is often ignored in beam/plate models. The through-the-thickness variations of the transverse deflection (Fig. 4) indicate that maximum core compression occurs at the midplane of the core where

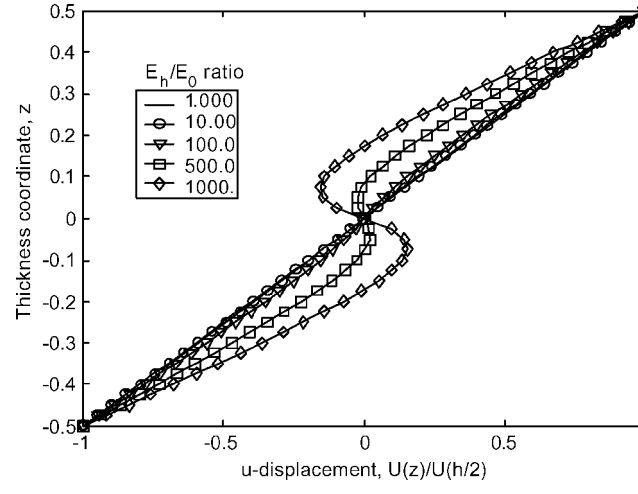

Fig. 3 Variation of in-plane displacement U through the thickness of the FGM beam for different ratios (E_h/E_0) at E_f/E_0 = 1000 (E_f, face-sheet modulus; E_h, sandwich core modulus at face-sheet interface; E_0, sandwich core modulus at center).

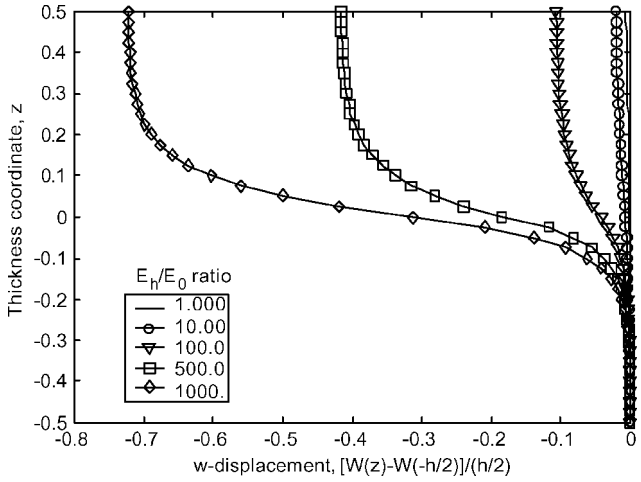

Fig. 4 Variation of transverse displacement W through the thickness of the FGM beam for different ratios (E_h/E_0) at E_f/E_0 = 1000 (E_f, face-sheet modulus; E_h, sandwich core modulus at face-sheet interface; E_0, sandwich core modulus at center).

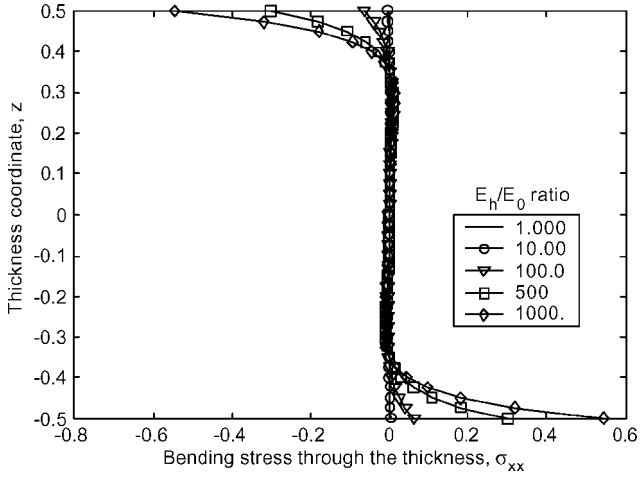

Fig. 5 Variation of the through-the-thickness bending stress (normalized by the face-sheet elastic modulus E_f) in the FGM beam for different ratios (E_h/E_0) at E_f/E_0 = 1000 (E_h, sandwich core modulus at face-sheet interface; E_0, sandwich core modulus at center).

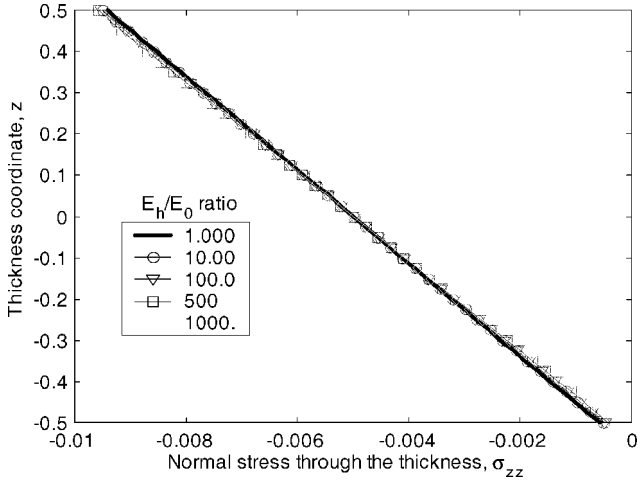

Fig. 6 Variation of the through-the-thickness normal compressive stress (normalized by the facesheet elastic modulus E_f) in the FGM beam for different ratios (E_h/E_0) at E_f/E_0 = 1000 (E_h, sandwich core modulus at face-sheet interface; E_0, sandwich core modulus at center).

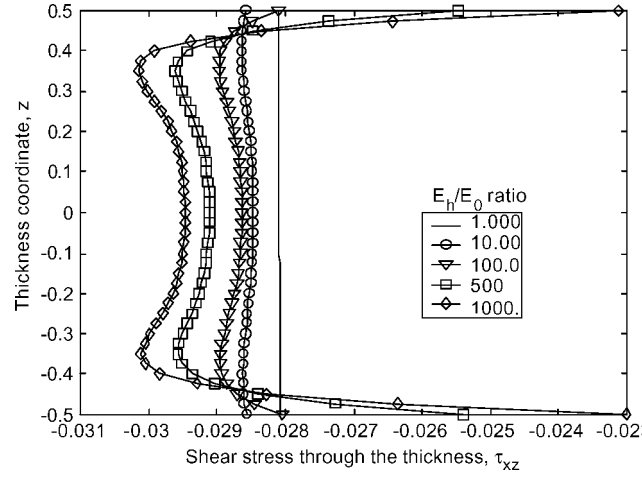

Fig. 7 Variation of the through-the-thickness shear stress (normalized by the face-sheet elastic modulus E_f) in the FGM beam for different ratios (E_h/E_0) at E_f/E_0 = 1000 (E_f, face-sheet modulus; E_h, sandwich core modulus at face-sheet interface; E_0, sandwich core modulus at center).

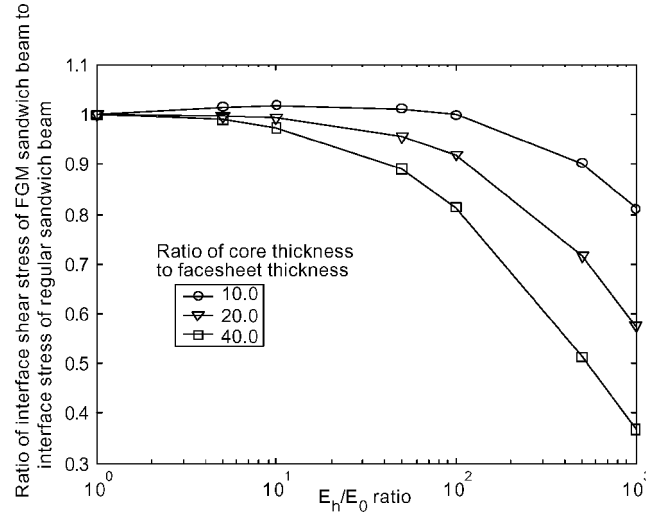

Fig. 8 Reduction in interfacial shear stresses for varying ratios of extreme values of core moduli (E_h/E_0) and ratios of core thickness to face-sheet thickness, h/h_f.

the elastic modulus is a minimum. The core compression increases as the E_h/E_0 ratio is increased.

The bending stress variations (Fig. 5) in the core are as expected. The linear variation in strains results in small levels of bending stress in the core near the midplane. The stress increases near the face sheet. This is particularly pronounced as the value of the core modulus is increased to match the value of the face-sheet thickness.

The normal stress σ_{zz} in the core (Fig. 6) varies linearly from the applied surface load on the top surface to zero at the bottom of the core, and this behavior seems to be independent of the variation in core properties. This is an interesting result because it simplifies the calculations required to study the core crushing problem. It must be noted that the example considered here used a smoothly varying (sinusoidal) surface pressure load. The results will need to be verified for concentrated loads such as contact loads.

The more interesting result from the present analysis is the transverse shear stresses at the core–face-sheet interface. Conventional design of sandwich laminates restrict the shear stress at the core–face-sheet interface to the bond (adhesive) shear strength, which is typically lower than the shear strength of the core material. Therefore, the core material is not fully utilized. It is hence desirable to reduce the interfacial shear stress while carrying a high shear stress in the core. It appears that this is possible with a functionally graded

core. The shear stress variations in the core are plotted in Fig. 7 for $h/h_f = 10$. The interface shear stress reduces as the E_h/E_0 ratio is increased. The maximum reduction of 20% occurs for the case $E_h/E_f = 1$, for which the core elastic modulus varies exponentially from $E_0 = E_f/1000$ at the center to $E_h = E_f$ at the core–face-sheet interface. Figure 8 shows the ratio of shear stress at the interface for different values of E_h/E_0 ratio and h/h_f ratio. The reduction in shear stress at the interface increases with increase in h/h_f ratio (or for beams when the face sheet is significantly thinner than the core). For the example problem the reduction in interface shear stress is 42 and 63% for h/h_f values of 20 and 40, respectively.

Summary

The elasticity solution obtained for a simple functionally graded beam has been extended for a sandwich configuration. The stresses calculated from the elasticity solution were used to demonstrate the reduction in face-sheet–core interface shear stress possible by functionally grading the sandwich core elastic properties.

Acknowledgments

This research was supported by NASA Langley Research Center Grant NAG-1-1887 to the University of Florida. The authors are thankful to D. R. Ambur, Head, Mechanics and Durability Branch, for his input and encouragement.

Reference

[1]Sankar, B. V., "An Elasticity Solution for Functionally Graded Beams," *Composites Science and Technology*, Vol. 61, No. 5, 2001, pp. 689–696.

K. N. Shivakumar
Associate Editor

Triangular Shell Element for Large Rotations Analysis

R. Levy*
Technion—Israel Institute of Technology, 32000 Haifa, Israel
and
E. Gal†
Ben Gurion University of the Negev, 84105 Beer Sheva, Israel

I. Introduction

GEOMETRICALLY nonlinear analysis of shells for small strains and large rotations can be described in terms of three key steps: derivation of the geometric stiffness matrix, iterative solution of the governing equations, and stress retrieval and updating. It is the derivation of the geometric stiffness matrix and stress retrieval for thin shells that is the focus of this Note. Here the geometry of the shell surface is approximated with flat triangular shell elements, each of which is composed of a membrane and a plate element.

In the literature a number of methods exist for the derivation of the geometric stiffness matrix of shells. These are based on classical nonlinear shell theory represented as a two-dimensional Cosserat surface, three-dimensional elasticity degenerate shells, and perturbation methods. The excellent comprehensive review by Ibrahimbegović[1] addresses the various approaches and the related complex issues involved.

The present approach is based on gradient methods that are equivalent to perturbation methods (e.g., Green et al.[2]), where first-order perturbation analysis corresponds to first-order Taylor-series linearization. Related to the present approach is the corotational realm (for example, see Bathe and Ho[3] and Peng and Crisfield[4]).

The geometric stiffness matrix is derived by first performing a load perturbation on the linear equilibrium shell equations with respect to the local coordinates system to yield the in-plane geometric stiffness matrix. Then out-of-plane considerations that involve the effect of rigid-body rotations on member forces complete the local geometric stiffness matrix formulation. As for stress retrieval, the linear equations of elasticity are used throughout because of the a priori removal of rigid-body rotations by a special procedure, which is developed later. These two features make this approach unique compared to other methods of similar general characteristics. Finally a computer program featuring incremental analysis and Newton's method, geometric effects, pure deformations isolation, internal stresses retrieval, and updating of nodal forces and coordinates was coded to implement the derivations described herein and used to solve a number of problems that appeared in the literature with practically matching results.

II. Geometric Stiffness Matrix of the Flat Triangular Shell Element

Load perturbation of the shell equilibrium equations leads to the well-established definition of the geometric stiffness matrix as the gradient with respect to the global coordinates of the nodal force vector when stresses are held fixed.[5] To circumvent the taking of impossible derivatives of the three-dimensional rotation matrix, the load perturbation method is applied with respect to local coordinates. In that case an additional out-of-plane effect has to be considered. This out-of-plane effect is physically the change in the nodal force vector as a result of the rigid-body rotation. The geometric stiffness matrix is thus composed of four individual matrices, two in-plane (IP) and two out-of-plane (OP) matrices for the membrane and plate elements, respectively:

$$\left[\boldsymbol{K}_G^e\right]_{\text{TOTAL}}^{\text{shell}} = \left[\boldsymbol{K}_G^e\right]_{\text{IP}}^{\text{mem}} + \left[\boldsymbol{K}_G^e\right]_{\text{IP}}^{\text{plate}} + \left[\boldsymbol{K}_G^e\right]_{\text{OP}}^{\text{mem}} + \left[\boldsymbol{K}_G^e\right]_{\text{OP}}^{\text{plate}} \tag{1}$$

A. In-Plane Contribution of the Flat Triangular Membrane Element

The nodal force vector of the simple plane stress triangular finite element (CST) that is described by Zienkiewicz[6] is used as the membrane element is given as

$$\boldsymbol{F}^e = \frac{t}{2}\begin{Bmatrix} b_i\sigma_x + c_i\tau_{xy} \\ c_i\sigma_y + b_i\tau_{xy} \\ \vdots \\ b_j\sigma_x + c_j\tau_{xy} \\ c_j\sigma_y + b_j\tau_{xy} \\ \vdots \\ b_m\sigma_x + c_m\tau_{xy} \\ c_m\sigma_y + b_m\tau_{xy} \end{Bmatrix} \begin{matrix} \\ \text{row } i \\ \\ \\ \text{row } j \\ \\ \\ \text{row } m \end{matrix} \tag{2}$$

where the coefficients b_r, c_r $r = i, j, m$ are explicitly defined in Ref. 6; t is the thickness of the element; and σ_x, σ_y, τ are its stresses. The gradient of Eq. (2) that is taken in a rather straightforward manner[6] to yield a 6×6 in-plane contribution to the geometric stiffness matrix of the membrane is

$$\left[\boldsymbol{K}_G^e\right]_{\text{IP}}^{\text{mem}} = \nabla \boldsymbol{F}_{\text{mem}}^e = \begin{bmatrix} \boldsymbol{0} & \boldsymbol{A}_{\text{IP}}^{\text{mem}} & -\boldsymbol{A}_{\text{IP}}^{\text{mem}} \\ -\boldsymbol{A}_{\text{IP}}^{\text{mem}} & \boldsymbol{0} & \boldsymbol{A}_{\text{IP}}^{\text{mem}} \\ \boldsymbol{A}_{\text{IP}}^{\text{mem}} & -\boldsymbol{A}_{\text{IP}}^{\text{mem}} & \boldsymbol{0} \end{bmatrix}$$

$$\boldsymbol{A}_{\text{IP}}^{\text{mem}} = \frac{t}{2}\begin{bmatrix} -\tau & \sigma_x \\ -\sigma_y & \tau \end{bmatrix} \tag{3}$$

Received 19 June 2002; revision received 7 July 2003; accepted for publication 24 July 2003.

*Associate Professor, Faculty of Civil and Environmental Engineering; cvrlevy@tx.technion.ac.il. Member AIAA.

†Postdoctoral Fellow, Department of Structural Engineering, Faculty of Engineering.